International Journal of Pharmaceutics 425 (2012) 19–28

Contents lists available at SciVerse ScienceDirect

International Journal of Pharmaceutics

journal homepage: www.elsevier.com/locate/ijpharm

Antitumor activities of emulsion electrospun fibers with core loading of hydroxycamptothecin *via* intratumoral implantation

Xiaoming Luo [1], Chengying Xie [1], Huan Wang, Chaoyu Liu, Shili Yan, Xiaohong Li *

Key Laboratory of Advanced Technologies of Materials, Ministry of Education of China, School of Materials Science and Engineering, Southwest Jiaotong University, Chengdu 610031, PR China

ARTICLE INFO

Article history:
Received 27 September 2011
Received in revised form
12 December 2011
Accepted 7 January 2012
Available online 14 January 2012

Keywords:
Emulsion electrospinning
Release modulation
Structural integrity
Intratumoral implantation
Antitumor activity

ABSTRACT

Emulsion electrospinning was used in the present study to prepare core–sheath structured fibers with core-loading of hydroxycamptothecin (HCPT), and their antitumor activities were evaluated both *in vitro* on cancer cell lines and *in vivo* on tumor bearing mice *via* intratumoral implantation. Compared with our previous investigation on blend electrospun fibers, the addition of 2-hydroxypropyl-β-cyclodextrin (HPCD) and the preferential formation of HPCT/HPCD inclusion complexes resulted in significantly faster HCPT release from and higher degradation rate of emulsion electrospun fibers. The core–sheath structure led to around 93% of lactone form remaining after emulsion electrospinning and incubation in buffer solutions for over one month. *In vitro* cytotoxicity tests on HCPT-loaded electrospun fibers indicated over 20 times higher inhibitory activity against HepG2 cells than free HCPT during 72 h incubation. Hepatoma H22 cells were subcutaneously injected into Kunming mice to form solid tumors for *in vivo* tests on the antitumor efficacy. Based on the tumor volume, survival rate and body weight changes, HCPT-loaded fibers indicated superior *in vivo* antitumor activities to and fewer side effects than free HCPT. The histopathological staining and immunohistochemical examinations of caspase-3 expression indicated more necrosis and apoptosis induced by HCPT-loaded fibers. The above results demonstrate the potential use of emulsion electrospun fibers as drug carriers for local treatment of solid tumors.

1. Introduction

Electrospinning affords great flexibility in producing polymer fibers with diameters ranging from a few nanometers to several micrometers using polymer solutions or melts. Ultrafine fibers formed by this technology have a large surface area, ensuring a high therapeutics take-up, and a three-dimensional open porous structure, which can reduce the constraint to drug diffusion leading to an increase in the total fraction of drug that can be released (Greiner and Wendorff, 2007). In addition, relevant fiber properties, such as the fiber size, porosity, drug loading and release mechanisms are highly customizable through process parameters and material choice, leading to a possibility to tailor the drug release rate for each application (Sill and von Recum, 2008). Lipophilic drugs such as rifampin and paclitaxel, hydrophilic drugs such as tetracycline hydrochloride and doxorubicin hydrochloride, and biomacromolecules such as protein and DNA have been encapsulated into electrospun fibers (Liang et al., 2007). But it is still challenging to maintain the structural stability and bioactivity of the encapsulated therapeutics, and achieve a defined release rate over a definite time in a controlled principle (Hadjiargyrou and Chiu, 2008).

When using electrospun fibers as drug carriers, the loading strategy of therapeutics within the fiber matrix is critical to modulate the loading capabilities and the release control mechanisms to operate. The loading methods can be generally categorized into entrapment and binding, dependent on the polymer carriers and therapeutics. Surfaces of electrospun fibers have been chemically functionalized for achieving sustained delivery through physical adsorption, layer-by-layer assembly of polyelectrolytes, or chemical immobilization of diverse bioactive molecules onto the fiber surface (Yoo et al., 2009). The entrapment of therapeutics into fibers has been realized through blend electrospinning, coaxial electrospinning and emulsion electrospinning. The major disadvantages of blend electrospinning are the severe burst release and the reducing of effective lifetime of the device (Luu et al., 2003). Coaxial electrospinning was adopted to encapsulate protein into poly(ε-caprolactone) fibers, indicating an initial burst release accounted for 45–65% of protein encapsulated (Zhang et al., 2006). It was noted that the electrohydrodynamic behaviors of coaxial electrospinning were complex, and the flow rates of the sheath and core solutions should be delicately tuned for steady co-axial jet formation during electrospinning. Otherwise, the possibility of jet break-up

* Corresponding author. Tel.: +86 28 87634068; fax: +86 28 87634649.
E-mail addresses: xhli@swjtu.edu.cn, xiaohongli@hotmail.com (X. Li).
[1] The authors contributed equally to the work.

0378-5173/$ – see front matter © 2012 Elsevier B.V. All rights reserved.
doi:10.1016/j.ijpharm.2012.01.012

and deposition of fibers without a uniform core or sheath layer is high due to differences in the conductivities and viscosities of the two solutions (Chakraborty et al., 2009). Alternatively, electrospun fibers with integral core–sheath structure have been prepared by emulsion electrospinning, where the emulsion droplets are stretched into an elliptical shape in the direction of the fiber trajectory. The rapid elongation and solvent evaporation during the electrospinning enhance their enrichment of droplets in the axial region. It is the viscosity difference between the elliptical droplets and the polymer matrix that directs core materials to settle into the fiber interior rather than on the surface. The integral core–sheath structure is essential to alleviate the initial burst release, prolong the release period and maintain the structural integrity and bioactivity of therapeutics incorporated into electrospun fibers (Yang et al., 2008). An initially burst release as low as 14.0% was achieved for growth factors-loaded fibers, followed by gradual release for around 4 weeks, which enhanced skin regeneration for diabetic rats with dorsal wounds (Yang et al., 2011b).

Hydroxycamptothecin (HCPT) is known as topoisomerase-I inhibitors exhibiting high antitumor activities against a wide spectrum of human malignancies, such as lung, prostate, breast, colon, stomach, and ovarian carcinomas. But clinical application of HCPT is limited by its formulation and delivery problems, because HCPT is extremely insoluble in water and physiologically acceptable organic solvents, and has a chemically unstable lactone ring (Kunii et al., 2007). HCPT has been modified by chemical conjugation (Singer et al., 2001), or formulated into liposome, micelle, hydrogel or nanoparticles (Derakhshandeh et al., 2007). But the poor solubility resulted in a limited loading capability (Zhang et al., 2007), and a sharp burst release in such drug delivery devices (Opanasopit et al., 2006). In addition, all these formulations were usually administered intravenously, which led to only a fraction of the total dose reached the tumor site, and a variety of undesirable side effects ranging from neutropenia to cardiomyopathy (Crawford et al., 2004). Drug-loaded electrospun fibrous mats show potentials as implantable device for cancer chemotherapy, for example, after surgical removal of solid tumors. The local regional delivery can be the optimal treatment for maximizing destruction to the tumor target by the enriched chemotherapeutic drugs, while limiting damage to the surrounding normal tissue by reducing the systemic dose (Pradilla et al., 2006). In our previous study HCPT was loaded into poly(DL-lactic acid)-poly(ethylene glycol) (PELA) fibers through blend electrospinning. *In vitro* cytotoxicity tests showed over 7 times higher inhibitory activity against cancer cells for HCPT-loaded electrospun fibers than free drug during 72 h incubation (Xie et al., 2010), but *in vivo* evidence for the inhibition efficacy on the tumor growth has not been provided to date.

In current study fibers with a core–sheath structure were used to entrap HCPT through emulsion electrospinning, which was supposed to protect the bioactivity and modulate the release of HCPT encapsulated. 2-Hydroxypropyl-β-cyclodextrin (HPCD) was included to enhance the structural integrity of HCPT, and modulate the drug release and matrix degradation of emulsion electrospun fibers. The antitumor activities of HCPT-loaded fibrous mats were evaluated both *in vitro* on cancer cell lines and *in vivo* on hepatic H22 tumor bearing mice *via* intratumoral implantation.

2. Materials and methods

2.1. Materials

Poly(ethylene glycol) (PEG, M_w = 6 kDa) was purchased from Sigma–Aldrich Inc. (St. Louis, MO). PELA containing 10% of PEG were prepared by bulk ring-opening polymerization using stannous chloride as initiator (Deng et al., 1999). HCPT was obtained from Sichuan Natural Product Co. (Chengdu, China), and HPCD, dimethylsulfoxide (DMSO) and bovine serum albumin (BSA) were from Sigma–Aldrich Inc. (St. Louis, MO). Rabbit anti-mouse antibody of caspase-3, goat anti-rabbit IgG-horseradish peroxidase (HRP) and 3,3′-diaminobenzidine (DAB) developer were purchased from Biosynthesis Biotechnology Co., Ltd. (Beijing, China). Ultrapure water from a Milli-Q biocel purification system (UPI-IV-20, Shanghai UP Scientific Instrument Co., Shanghai, China) was used. All other chemicals and solvents were of reagent grade or better, and purchased from Changzheng Regents Co. (Chengdu, China) unless otherwise indicated.

2.2. Preparation of HCPT-loaded electrospun fibers

HCPT was dissolved in DMSO and suspended in aqueous solution of HPCD, which was emulsified in PELA solution in methylene chloride, followed by emulsion electrospinning as described elsewhere (Yang et al., 2011a). Briefly, 80 μl of HCPT solution in DMSO and 80 μl of HPCD aqueous solution were mixed together and vortexed for 30 s. The suspension was emulsified into 3.0 ml of methylene chloride containing 450 mg of PELA. The resulting emulsion was added in a 5 ml-syringe attached to a metal capillary, and a steady flow at 1.6 ml/h out of the capillary was controlled by a microinject pump (Zhejiang University Medical Instrument Co., Hangzhou, China). The electrospinning apparatus was equipped with a high-voltage statitron (Tianjing High Voltage Power Supply Co., Tianjing, China), and the applied voltage was set as 20 kV. Fibers with HCPT loading amount of 1.0% and 3.0% and HPCD additions of 0.5%, 1.0% and 1.5% were prepared. The collected fibers were lyophilized overnight to remove any solvent and water residues and stored at 4 °C away from light.

2.3. Characterization of HCPT-loaded electrospun fibers

The morphology of electrospun fibers were observed by scanning electron microscope (SEM, FEI Quanta 200, The Netherlands) equipped with accelerating voltage (20 kV) and Robinson detector after 2 min of gold coating to minimize charging effect. The fiber diameter was measured from SEM images by using photoshop v8.0 as described previously (Cui et al., 2006). HCPT is highly fluorescent, and the distribution of HCPT in electrospun fibers was examined by a laser confocal scanning microscope (LCSM, Leica TCS SP2, Germany) with the excitation and emission wavelengths of 418 nm and 515 nm, respectively. A superimposing of the fiber image without excitation on the same fiber image with excitation provided a representation of the fiber structure (Yang et al., 2011a).

The loading efficiency of HCPT was determined after being extracted from electrospun fibers (Xie et al., 2010). Briefly, a known amount of fibers were dissolved in 1.0 ml chloroform and extracted three times with 20.0 ml pH 7.4 phosphate buffer saline (PBS). The extract solution was detected by a fluorospectrophotometer (Hitachi F-7000, Japan) with the excitation wavelength of 380 nm and the emission wavelength of 550 nm, in which HCPT concentration was obtained using a standard curve from known concentrations of HCPT solutions. The extraction efficiency was calibrated by adding a certain amount of HCPT into polymer/chloroform solution along with the same concentration as above and extracted using the above-mentioned process. The encapsulation efficiency, determined in triplicate for at least five different batches, indicated the percentage of HCPT encapsulated with respect to the total amount used for the fiber preparation.

The structural stability of HCPT that remained in ultrafine fibers was determined by reverse-phase high-performance liquid chromatograph (HPLC) (Li and Zhang, 1996). Briefly, HPLC (Waters 2695, Milford, MA) was operated with ultraviolet detector set at 266 nm and C18 column (4.6 mm × 150 mm) at 40.0 °C. The mobile phase

was 40/60 (v/v) of pure water and methanol (Fisher Scientific, Fair Lawn, NJ) at a flow rate of 1.0 ml/min. The drug-loaded fibers were dissolved in methylene chloride, extracted with the mobile phase, and the supernatant was analyzed by HPLC immediately. The retention time of the carboxylate form of HCPT was 1.7–2.0 min, while that of the lactone form was 3.0–3.5 min. The peak areas were measured, and the actual contents were calibrated using a standard curve from known concentrations of HCPT solutions. Stock solutions of HCPT in DMSO were diluted with buffer solutions of pH values of 3.0 and 9.0 to obtain HCPT of the lactone and carboxylate forms, respectively.

2.4. In vitro drug release and matrix degradation of HCPT-loaded electrospun fibers

The drug release profiles were determined on fibrous mats with HCPT loadings of 1% and 3%, HCPD additions of 0.5%, 1.5% and 2.5%. Drug-loaded fibrous mats with corresponding to around 120 μg HCPT were exactly weighed and immersed in 40.0 ml PBS (pH 7.4) to ensure a sink condition. All these suspensions were kept in a thermostated shaking water bath which was maintained at 37 °C and 120 cycles/min. At predetermined time intervals, 1.0 ml of the released solution was removed for analysis, and equal amount of fresh buffer solution was added back. The HCPT concentration in the release media was detected by a fluorospectrophotometer as described above.

The degradation profiles of HCPT-loaded fibers were determined with respect to the molecular weight reduction and mass loss, compared with PELA fibers and fibers containing HPCD. Preweighed fibrous mats were incubated at 37 °C in 20.0 ml PBS (pH 7.4) containing 0.02% sodium azide as a bacteriostatic agent. At predetermined time intervals, a group of each fibrous mat was retrieved and rinsed with pure water to eliminate residual buffer salts, and dried in a vacuum desiccator to maintain a constant weight. The mass loss was determined gravimetrically by comparing the dry weight remaining at a specific time with the initial weight. The molecular weight of recovered matrix polymers was determined by gel permeation chromatograph (GPC, Waters 2695 and 2414, Milford, MA) with a Styragel HT 4 column (7.8 mm × 300 mm) using polystyrene beads as standard. Tetrahydrofuran (THF, Fisher Scientific, Fair Lawn, NJ) was used as the mobile phase at a flow rate of 1.0 ml/min.

2.5. In vitro cytotoxicity assay of HCPT-loaded electrospun fibers

The inhibition of cancer cell growth was assayed with cell counting kit-8 reagent (CCK-8, Dojindo Molecular Technologies, Inc., Kumamoto, Japan) after treatment with drug-loaded fibers, compared with free HCPT. Human hepatocellular carcinoma cells HepG2 were obtained from the American Type Culture Collection (Rockville, MD), and cultured in RPMI 1640 (Gibco BRL, Rockville, MD) containing 10% fetal bovine serum (FBS, Gibco BRL, Rockville, MD) and 100 U/ml pencillin and 100 μg/ml streptomycin (Sigma, St. Louis, MO). Briefly, the cell density of 1×10^4 cells/ml was seeded in 48-well tissue culture plate (TCP), and allowed 24 h to attach and grow in wells before drug treatment. HCPT-loaded electrospun fibers were exactly weighed by a microbalance (Sartorius SE2, Goettingen, Germany), sterilized by electron-beam irradiation using linear accelerator (Precise™, Elekta, Crawley, UK) with a total dose of 80 cGy, and put into above wells. The HCPT stock solution was diluted in RPMI 1640, and drug-loaded electrospun fibers releasing equivalent amount of HCPT during 72 h (from *in vitro* release data) were applied. PELA fibers without drug inoculation were also tested. After incubation for 72 h, all the groups were washed by fresh media twice, and filled with 300 μl of RPMI 1640 containing 30 μl CCK-8 in each well and incubated for 3 h according to the reagent instruction. An aliquot (150 μl) of incubation medium was pipetted into a 96-well TCP, and the absorbance at 450 nm was measured for each well by a microplate spectrophotometer (Elx-800, Bio-Tek Instrument Inc., Winooski, VT).

2.6. Establishment of H22 tumor bearing mice model

All animal procedures were approved by the University Animal Care and Use Committee. Mouse hepatoma H22 cells were kindly gifted by the state key laboratory of biotherapy of Sichuan University (Chengdu, China), and 6–8 week old Kunming mice weighing 18–22 g were supplied by Sichuan Dashuo Biotech Inc. (Chengdu, China). The tumor model was established subcutaneously as described previously with some modifications (Xiong et al., 2005). Briefly, H22 cells were suspended in physiological saline and injected intraperitoneally into the mice for serial subcultivation. Then the mice with viable H22 ascites tumors were sacrificed, and the ascites was withdrawn and diluted with physiological saline to modulate the cell density at 1×10^7 cells/ml. The ascites was injected subcutaneously to each animal at the left axilla at a dose of around 10 μl/g body weight. The tumor cells were allowed to grow for around 10 days, and the mean tumor size at the initiation of therapy was $515.7 \pm 39.2\ mm^3$.

2.7. Intratumoral implantation of HCPT-loaded fibrous mats

The inhibition of tumor growth was determined after implantation of HCPT-loaded fibrous mats into established rumors. Briefly, tumor bearing mice were randomly divided into four groups with 8 animals in each group, which were treated with HCPT-loaded fibrous mats, empty electrospun fibers, free HCPT, and saline as control. The HCPT dose was equivalent to the total amount of 4.0 mg/kg. Animals were anesthetized by intraperitoneal injection of pentobarbital at 25 mg/kg, and the hair was removed with hair clippers. A small incision was made on the skin to expose the tumor, and then a small incision was made into the tumor. Fibrous mats were well inserted into the tumor, and the wound was closed using subcutaneous suturing. Free HCPT was formulated into PBS containing DMSO (5%, v/v), and each animal was administrated about 0.2 ml into the tumor.

The inhibition of tumor development was determined after tumor cell injection in the presence of HCPT-loaded fibrous mats, using empty electrospun fibers as control. Briefly, after animals were anesthetized small incisions were made in the back using a blade, and small subcutaneous pockets were created by incision using blunt scissors. After subcutaneous implantation of fibrous samples, incisions were closed and allowed to heal for 2 days before tumor cell injection to avoid leakage of the cells. The ascites containing H22 cells of 1×10^7 cells/ml was injected on the fibrous mats at a dose of around 10 μl/g body weight. The local tumor growth was defined as the development of subcutaneous tumor nodules overtop the implanted fibers with and without HCPT loading (Wolinsky et al., 2010).

2.8. Determination of tumor growth inhibition

The body weights, tumor volumes and survival rate of animals were monitored every other day after treatment. The length of the major axis (longest diameter) and minor axis (perpendicular to the major axis) of the tumor were measured with vernier calipers, and the tumor volumes (V) were calculated by the formula (Li et al., 2008):

$$V = \frac{l w^2}{2},$$

where l and w represent lengths of the major and minor axis of the tumor, respectively. The relative tumor growth (RTG) was calculated as following equation:

$$\mathrm{RTG}\,(\%) = \frac{(V_t - V_0)}{V_0} \times 100\%,$$

where V_t and V_0 are the volumes of tumors at time t and day 0, respectively.

2.9. Histological and immunohistochemical examinations on tumors retrieved

At day 14 after treatment animals were euthanized to retrieve tumors, which were fixed in 10% neutral buffered formalin. The tissues were processed routinely into paraffin blocks, sectioned at a thickness of 4 μm, stained with hematoxylin and eosin (HE) according to the standard histological technique, and observed with a light microscope (Nikon Eclipse E400, Japan). To investigate the apoptosis of tumor cells after treatment, immunohistochemistry assessment of caspase-3 expression was conducted on tumor tissues. Briefly, paraffin sections were incubated with 3% H_2O_2 for 10 min to inactivate endogenous peroxidase. To recover antigen, these sections were put into 10 mM citrate buffer solution (pH 6.0) and heated in a microwave oven twice, followed by washing twice with PBS. Non-specific binding sites were blocked with 5% BSA in Tris-buffered saline for 20 min. After the redundant liquid was discarded, the sections were incubated with primary caspase-3 antibody at 4 °C overnight and washed with PBS. Then the slides were incubated with biotinylated secondary antibody for 20 min, followed by incubation with streptavidin-HRP for 20 min. The antibody binding sites were visualized by incubation with a DAB–H_2O_2 solution. The slides were counterstained for 1 min with hematoxylin and then dehydrated with sequential ethanol for sealing and microscope observation. The expression levels of caspases-3 were compared by quantity of apoptotic cells/100 cells by 200× magnification of five different areas.

2.10. Statistics analysis

Data are expressed as mean ± standard deviation (S.D.). The statistical significance of the data obtained was analyzed by the Student's t-test. Probability values of $p < 0.05$ were interpreted as denoting statistical significance.

3. Results and discussion

3.1. Characterization of HCPT-loaded electrospun fibers

Fig. 1a shows SEM morphologies of HCPT-loaded electrospun fibrous mats, which possessed the common feature of porous, bead-free and randomly arrayed. The diameters were about 540 ± 70 nm. Fig. 1b shows the fluorescence of drug-loaded fibers under excitation, suggesting the presence of HCPT in electrospun fibers. Inset of Fig. 1b gives a representation image of the same fiber with or without excitation superimposed on one another, showing a core–sheath structure. The immiscibility of the aqueous and organic phases of the emulsion led to sharp boundaries between the two phases, which was essential to form core–sheath structured fibers through emulsion electrospinning (Yu et al., 2004). On the other hand, the immiscibility of the aqueous and organic phases caused the instability of the emulsion. Therefore, in current study HPCD was added to improve the emulsion stability and enhance the drug encapsulation during the emulsion electrospinning process. Efficient drug encapsulation was one of the advantages of electrospun fibers (Xie et al., 2010), and the addition of HPCD showed little influence on HCPT loading efficiency. There was over 95% of loading efficiency for fibers with up to 2.5% of HPCD inoculation and 1.0% or 3.0% of initial HCPT addition.

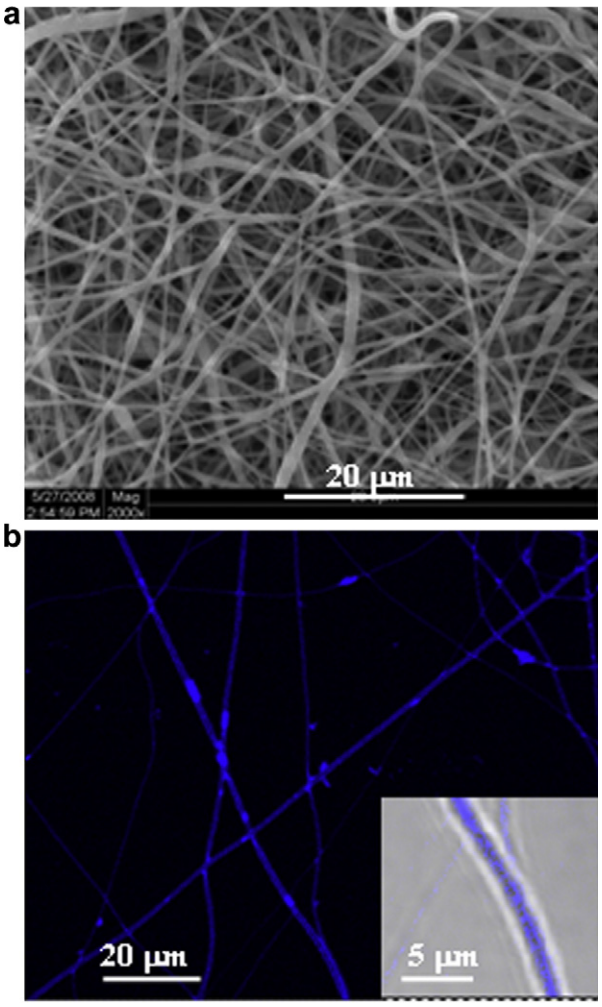

Fig. 1. SEM (a) and CLSM images (b) of HCPT/PELA fibers. Inset shows images of the same fiber with and without excitation superimposed on one another.

3.2. In vitro HCPT release profiles from electrospun fibers

For these extremely hydrophobic drugs, regulation of the release rate from polymer matrices is one of the challenges to maintain suitable drug concentration within a therapeutic window for enough exposure time. As shown in our previous study, there were around 15% of initial burst release for HCPT/PELA fibers, and no more release was detected during the following 20 day incubation (Xie et al., 2010). HPCD was included in the fiber matrix to enhance the constant release of such hydrophobic antineoplastic agents through adjusting the matrix degradation and scaffold microstructure. Fig. 2 shows the release profiles from emulsion electrospun fibers with HCPT loadings of 1.0% and 3.0% and HPCD inoculations of up to 2.5%. The release kinetics can be illustrated into two stages: An initial burst release followed by a constant release of up to 90% during 20 day incubation. Around 25% and 30% of burst release were indicated for fibers with 1.0% and 3.0% of HCPT loadings, respectively. Compared with around 15% of burst release from blend electrospun HCPT/PELA fibers with HPCD inoculations (Xie et al., 2010), the higher initial release from emulsion electrospun fibers was due to the distribution pattern of HPCD and HCPT within fibers. The randomly distributed HPCD within blend electrospun

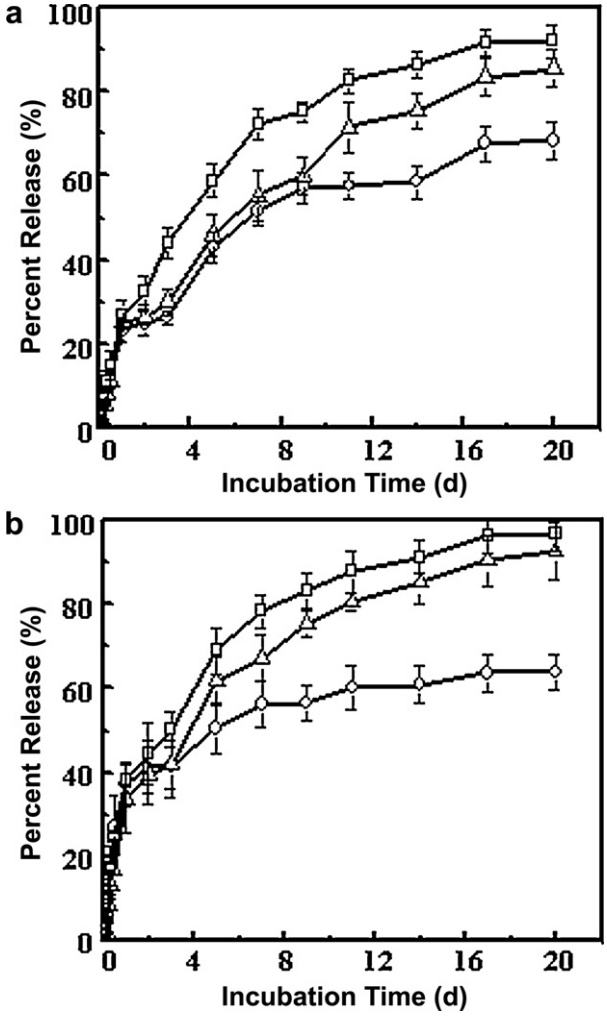

Fig. 2. *In vitro* drug release of electrospun fibers with HCPT loadings of 1% (a) and 3% (b) and containing 0.5% (○), 1.5% (△) and 2.5% HPCD (□) after incubation in pH 7.4 PBS at 37 °C ($n = 3$).

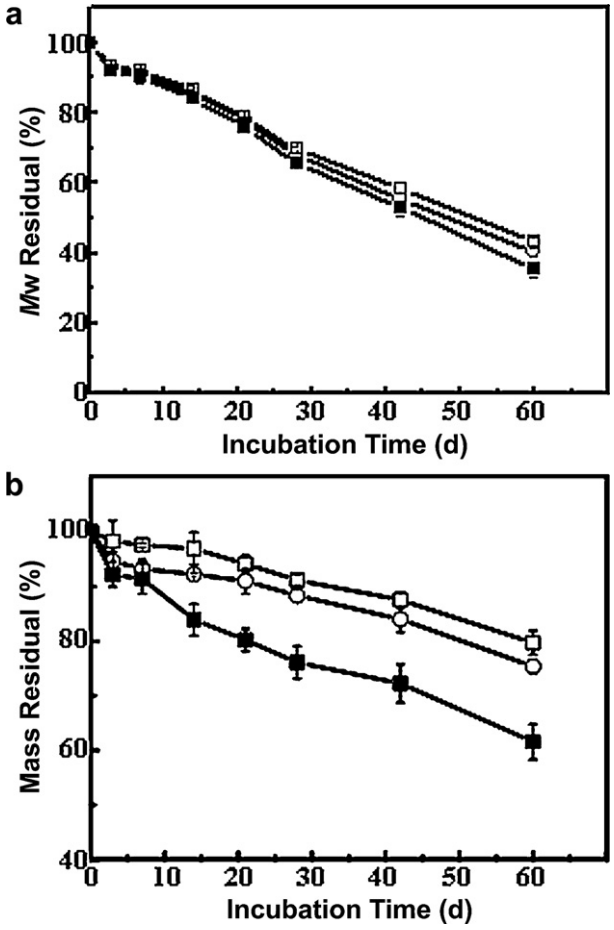

Fig. 3. The molecular weight reduction (a) and mass loss (b) of electrospun PELA fibers (○), PELA fibers containing 1.5% HPCD (□) and HCPT/PELA fibers containing 3% HPCT and 1.5% HPCD (■) after incubation in pH 7.4 PBS at 37 °C ($n = 3$).

fibers and interactions of hydrophobic HCPT with matrix polymers resulted in lower initial release during incubation. The preferential formation of HCPT/HPCD complexes resulted in a fast release from emulsion electrospun fibers. As shown in Fig. 2, no significant difference in the amount of initial burst release was found for HCPT/PELA fibers with different HPCD inoculations ($p > 0.05$). HPCD was indicated to be able to enhance the aqueous solubility and chemical stability of HCPT due to the formation of HCPT/HPCD inclusion complexes (Saetern et al., 2004). The addition of high amount of HPCD should facilitate the dissolution of HCPT enriched close to fiber surface during the electrospinning process or loosely associated with the fiber matrix. However, the improved emulsion stability after the addition of HPCD resulted in more integral core–sheath structure, leading to a decrease in the burst release. Therefore, the competitive effects of HPCD on the dissolution enhancement and the preferential distribution of HCPT/HPCD complexes within the fiber matrix resulted in no significant difference in the initial burst release from fibers with HPCD inoculations of 0.5%, 1.5% and 2.5%.

As shown in Fig. 2, significant differences were detected during the sustained release stage for HCPT/PELA fibers with different HPCD inoculations. When HPCD inoculations were increased from 0.5% to 2.5%, the cumulative release during 20 day incubation increased from 68.4% to 92.0% for fibers with 1.0% of HCPT loading, and from 63.8% to 96.6% for fibers with 3.0% of HCPT loading. There was no significant difference between fibers with 1.0% and 3.0% of HCPT loadings for each HPCD inoculation ($p > 0.05$). Hydrophilic HPCD should easily diffuse from fibers, and the liberated HPCD could be as effective solubilizing agents for HCPT to maintain a large concentration gradient for HCPT between the release media and the fiber matrix. Furthermore, the liberated HPCD or HCPT/HPCD complexes made lots of micropores, and the high surface area for diffusion throughout the ultrafine fibers allowed more HCPT to permeate from fiber matrices. Therefore, significantly larger HCPT release was indicated in the second phase for fibers with higher HPCD inoculations. As indicated previously (Xie et al., 2010), the total HCPT release from blend electrospun fibers with 1.0% of HCPT loading and 2.5% of HPCD inoculation were around 44.8%, which was significantly lower than 92.0% from the corresponding emulsion electrospun fibers ($p < 0.05$). This may be due to higher diffusion rates of HCPT/HPCD inclusion complexes within emulsion electrospun fibers than HCPT (Bibby et al., 2000). As indicated in Fig. 2, there was no significant disparity of HCPT release profiles between fibers with different HCPT loadings, and HCPT/PELA fibers with 3% of HCPT loading were used in the following *in vitro* and animal implantation study.

3.3. *In vitro degradation of HCPT-loaded electrospun fibrous mats*

Fig. 3 shows the molecular weight reduction and mass loss of HCPT-loaded fibers after incubation in buffer solutions, compared with PELA fibers and fibers containing HPCD. There was no significant disparity of the degradation profiles among electrospun fibers containing different amounts of HPCD (data not shown). As shown

in Fig. 3, there were around 24.6% and 59.6% of mass loss and molecular weight reduction, respectively, during 60 day incubation of electrospun PELA fibers. But a slower degradation rate was detected for electrospun PELA fibers with HPCD inoculations, at 20.3% and 56.9% of mass loss and molecular weight reduction, respectively. As indicated in our previous study, the electrospinning process led to hydrophobic fibrous surface of electrospun PELA fibers with the water contacting angle of $114.0 \pm 1.3^{\circ}$, which was much higher than that of casting film of $70.1 \pm 2.3^{\circ}$ (Cui et al., 2008). The high hydrophobicity and water repellent properties of electrospun PELA fibers prevented the diffusion of oligomers with carboxylic acid end groups, resulting in an autocatalysis effect during the degradation of electrospun PELA fibers. The addition of HPCD into the fiber matrix enhanced the water diffusion into and the oligomers diffusion out of the fiber matrix, which alleviated the autocatalysis effect and slowed down the degradation of electrospun PELA fibers with HPCD inoculations. As indicated previously, the mass loss and molecular weight reduction were 15.0% and 52.2% for blend electrospun PELA fibers with HPCD inoculations (Xie et al., 2010), which were significantly lower than emulsion electrospun PELA fibers containing HPCD. This was due to the less uniform distribution of HPCD within emulsion electrospun fibers, resulting in less significant alleviation of the autocatalysis effect.

As shown in Fig. 3, the entrapment of HCPT into the fibers matrix speeded up the degradation of the matrix polymer comparing with PELA fibers with HPCD inoculations, which may be attributed to the microstructure after drug release. There were around 38.5% and 64.6% of mass loss and molecular weight reduction, respectively, for HCPT-loaded fibers during 60 day incubation. Compared with blend electrospun fibers with mass loss of 23.4% and molecular weight reduction of 58.0%, the significantly higher degradation rate was due to the core–sheath structure of emulsion electrospun fibers. The dissolution of HCPT/HPCD inclusion complexes should leave more microporous frame on emulsion electrospun fibers compared with blend electrospun fibers, and the high contact area of fiber matrices with the degradation medium enhanced the degradation process. Moreover, HPCD was mainly distributed in the core of emulsion electrospun fibers, and the autocatalytic decomposition of the polymer sheath was more significant than the polymer matrix of blend electrospun fibers. On the other hand, the acidic microenvironment inside electrospun fibers was beneficial to maintain the structural stability of HCPT included.

3.4. Structural stability of HCPT in electrospun fibers

One of the challenges of HCPT formulation is the preservation of the lactone ring, which is crucial for their anti-tumor activities. The lactone ring hydrolyzes under physiological condition and exists in a pH-dependent equilibrium with an open carboxylate form, which shows less antitumor activity and several unpredictable side effects (Gabr et al., 1997). In addition, this equilibration is also affected by the preferential binding of serum albumin to the carboxylate form, resulting in more rapid opening of the lactone ring under physiological environment (Opanasopit et al., 2005). The structural stability of HCPT in the ultrafine fibers after electrospinning and incubation into the release medium was determined in current study. Fig. 4 summarizes the percent of lactone form of HCPT extracted from HCPT/PELA fibers containing different amounts of HPCD, in comparison with free HCPT, after incubation into buffer solutions. The amount of HPCD inoculated indicated no significant difference in the structural integrity for both HCPT/PELA fibers and free HCPT ($p > 0.05$). As shown in Fig. 4a, the percent of lactone ring of HCPT decreased along with the incubation in pH 7.4 PBS, and the half-life ($t_{1/2}$) of around 40 min was detected. The percentage of the lactone form was maintained around 93% after emulsion electrospinning, which was higher than that after blend electrospinning (Xie et al., 2010). The entire drug fraction retained its active lactone form in ultrafine fibers after incubation for over one month in buffer solutions (Fig. 4b). The surface of electrospun HCPT/PELA fibers was hydrophobic, and the core–sheath structure of emulsion electrospun fibers prevented from exposing to the liquid environment. Such insufficient water diffusion in electrospun fibers could not dissolve HCPT and arrest kinetically lactone–carboxylate conversion by preventing the favorable reaction occurrence. In addition, there may present a low microenvironmental pH inside ultrafine fibers along with the polymer degradation as discussed above, which can be a critical element for shifting the lactone–carboxylate equilibrium. It suggested that electrospun fibers could effectively release the lactone form of HCPT, which was crucial to the antitumor activities of HCPT-loaded fibers.

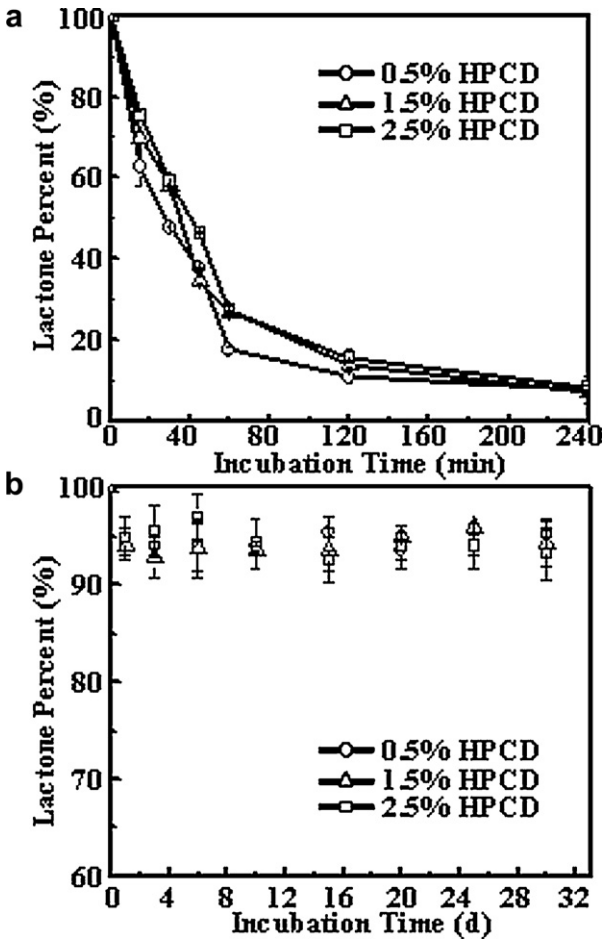

Fig. 4. The lactone percentage of free HCPT after incubation at 37 °C in pH 7.4 PBS containing HPCD (a) and HCPT extracted from HCPT/PELA fibers containing different amounts of HPCD (b) after incubation in pH 7.4 PBS at 37 °C ($n = 3$).

3.5. In vitro cytotoxicity assay of HCPT-loaded electrospun fibers

In vitro cytotoxicity of HCPT-loaded fibers was tested on HepG2 cells, and equivalent amount of HCPT was dosed for each kind of drug-loaded fibers corresponding to that released during 72 h. Free HCPT and empty PELA fibers were chosen as control. Fig. 5 summarizes the cell viability during 72 h incubation, and the half maximal inhibitory concentration (IC_{50}) was determined to show the effectiveness to inhibit the growth of tumor cells. As shown in Fig. 5a, IC_{50} of 1800 ng/ml was detected for free HCPT. As shown in Fig. 5b, there was no significant cell cytotoxicity for PELA fibers containing 1.5% of HPCD. However, the IC_{50} values of HCPT-loaded fibers with the HPCD additions of 0.5%, 1.5% and 2.5% were 47, 30 and 25 μg/ml,

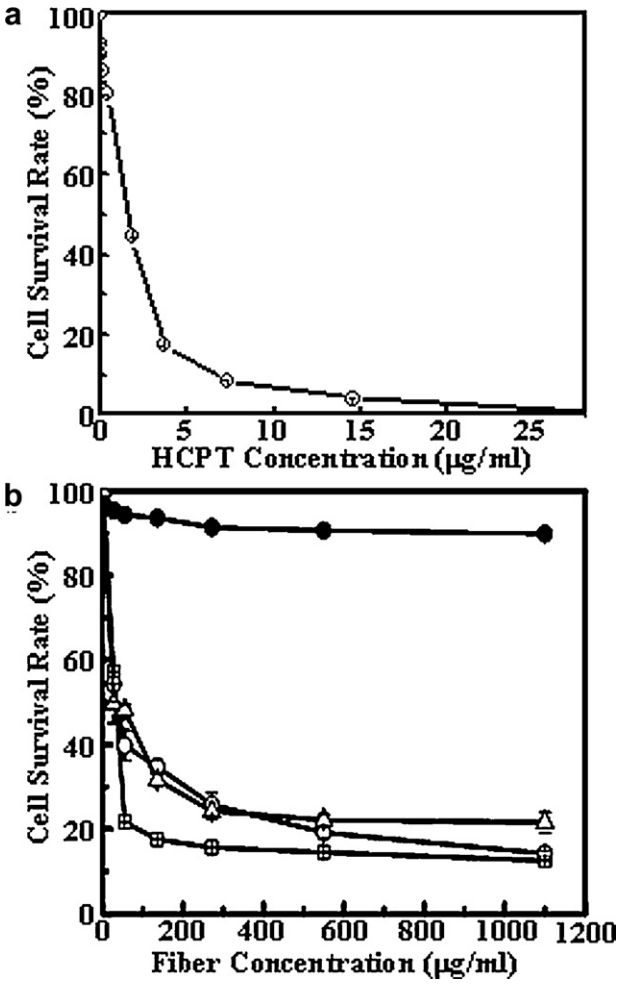

Fig. 5. *In vitro* cytotoxicity to HepG2 cells after treated by (a) free HCPT, (b) PELA fibers containing 1.5% HPCD (●), and HCPT/PELA fibers with 3% of HCPT loading and 0.5% (○), 1.5% (△) and 2.5% of HPCD inoculations (□) ($n = 5$).

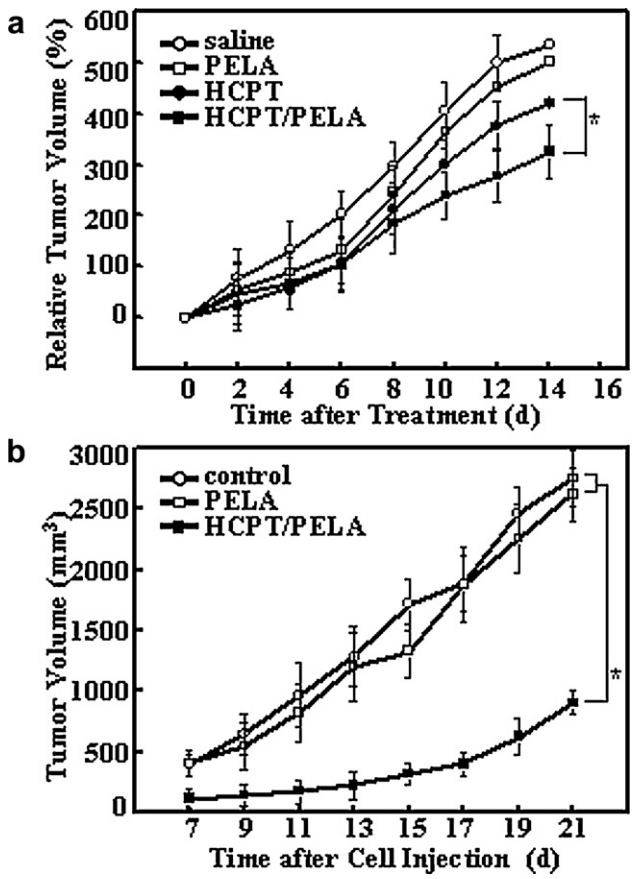

Fig. 6. (a) Percent increase in the tumor volume of H22 tumor bearing mice after intratumoral implantation of HCPT/PELA fibrous mats, empty PELA fibers, free HCPT and saline as control; (b) tumor growth after injection of H22 cancer cells on subcutaneously implanted HCPT/PELA fibrous mats, empty PELA fibers, using without any implantation as control. *: $p < 0.05$.

which equaled to around 87.0, 58.5 and 60.0 ng/ml of free HCPT, respectively. This showed over 20 times higher inhibitory activity against HepG2 cells than free HCPT. Blend electrospun fibers indicated around 7 times higher inhibitory activity than free HCPT in our previous study (Xie et al., 2010). The significantly higher inhibition effect on tumor cell growth may be attributed to the predominant protection of active lactone ring of HCPT during emulsion electrospinning process and the sustained release of its active form from electrospun fibers. In summary of the structural integrity (Fig. 4) and cytotoxicity results (Fig. 5), PELA fibers with 3% of HCPT loading and 1.5% of HPCD inoculation were applied for the antitumor efficacy study *via* intratumoral implantation.

3.6. Antitumor activities of HCPT-loaded fibrous mats

In recent years, liver cancer is still one of the most harmful diseases and a significant threat to the public health in China (Ding et al., 2011). In this study, H22 tumor bearing mice were chosen to evaluate the antitumor efficacy of HCPT-loaded fibrous mats with respect to the inhibition of tumor growth and development, and the survival rate of animals. The day when the drug treatments were initiated was day 0, and Fig. 6a summarizes the relative tumor growth curve after treatments with HCPT/PELA fibrous mats, empty PELA fibers, free HCPT and saline as control. Tumor volumes of the mice increased rapidly, and there was an over 5-fold increase after 14 day treatment with saline and empty PELA fibers. There was no significant difference in the tumor volume between saline and PELA fiber treatment at most of the time points ($p > 0.05$), indicating no apparent cytotoxicity of PELA fibers after intratumoral implantation. The tumor volume of free HCPT-treated mice increased about 420% during 14 day treatment. By comparison, there was around 256% increase in tumor volume observed in H22 tumor bearing mice treated with HCPT/PELA fibers, and significant differences were found compared with other groups ($p < 0.05$). As shown in Fig. 6a, the increase in the tumor volume of mice treated with saline, PELA fiber and free HCPT became accelerated after 6 days. The continuous inhibition of tumor growth after HCPT/PELA fiber treatment was due to the sustained release of HCPT from fibers.

As part of the clinical management of cancer, solid tumors are removed as much as possible from cancer patients, but it is difficult to completely remove the tumor through surgery (Pockaj and Gray, 2009). Thus, in many cases there is a local recurrence of tumors, initiated by residual cancer cells remaining at or near the resection margins or site of initial treatment (Bouchard and Efron, 2010). In the present study fibrous mats was subcutaneously implanted in health animals, and two days were allowed for the healing of the incision before cancer cells were injected on the fibrous mats. Fig. 6b shows the inhibition of tumor development after implantation of HCPT/PELA and empty PELA fibers, using without any implantation as control. After injection of H22 cells on HCPT/PELA fibrous mats, the tumor volumes reached around 117 mm^3 on day 7, which was significantly smaller than those of groups of empty PELA fibers and control ($p < 0.05$), with tumor volume of around 411 and 394 mm^3, respectively. As indicated in Fig. 6b, the tumors

on HCPT/PELA fibrous mats grew significantly slower than other groups during the following incubation. On day 21 after tumor cell injection there were around 5-fold increase for PELA fibers and control groups, with tumor volumes were around 2625 and 2755 mm^3, respectively. But a significantly smaller tumor of around 905 mm^3 was observed after cell injection on HCPT/PELA fibers ($p < 0.05$). This excellent antitumor efficacy can be attributed to the sustained release of HCPT from fibers and the retention of structural integrity of HCPT released from fibers.

3.7. Animal growth and survival rate after treatment

The survival rates of tumor-bearing mice after different treatment are plotted in Fig. 7a. The 4.0 mg/kg dose of free HCPT resulted in no difference in survival time compared to control group, and all of the mice died within 16 days. The diffusion of HCPT from tumors to other tissues may cause significant non-specific toxicity. Therefore, the survival period of tumor-bearing animals reflected not only the antitumor activity but also the toxicity of the treatment. All the mice died within 13 days after treatment with empty PELA fibers, and this was possibly because of the intervention by intratumoral implantation. However, the animals survived for 25 days after treatment with HCPT/PELA fibers. As shown in Fig. 7a, The median survival time for the groups receiving saline, empty PELA fibers, free HCPT and HCPT/PELA fibers was about 9, 8, 12 and 14 days, respectively, suggesting that the survival rates of tumor-bearing mice treated with HCPT-loaded fibers were significantly improved ($p < 0.05$). This may be resulted from the superior antitumor effect and reduced side effect of locally sustained release of HCPT from fibers.

In order to investigate the toxicity of different treatment, body weights were monitored every other day. Fig. 7b summarizes the results, indicating no significant difference in the body weight change among the groups. The body weight indicated less than

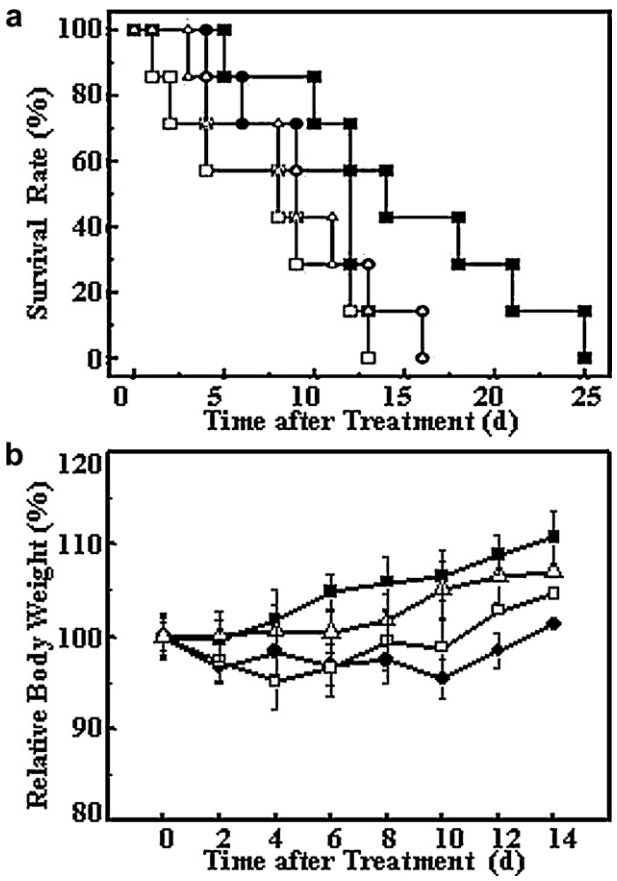

Fig. 7. Survival curve (a) and body weight changes (b) of H22 tumor bearing mice after intratumoral implantation of HCPT/PELA fibrous mats (■), empty PELA fibers (□), free HCPT (●) and saline as control (△).

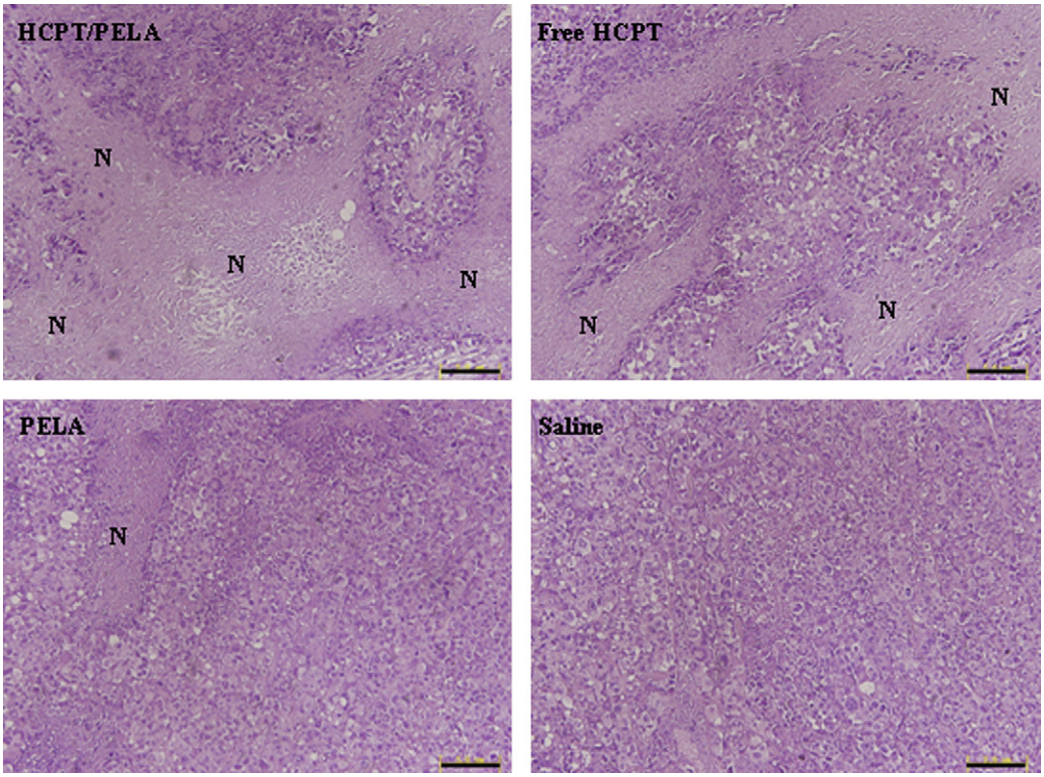

Fig. 8. Typical HE staining images of tumors retrieved on day 14 after treatment with HCPT/PELA fibrous mats, empty PELA fibers, free HCPT and saline as control. *N* represents necrotic area. Bars represent 100 μm. (For interpretation of the references to color in the text, the reader is referred to the web version of the article.)

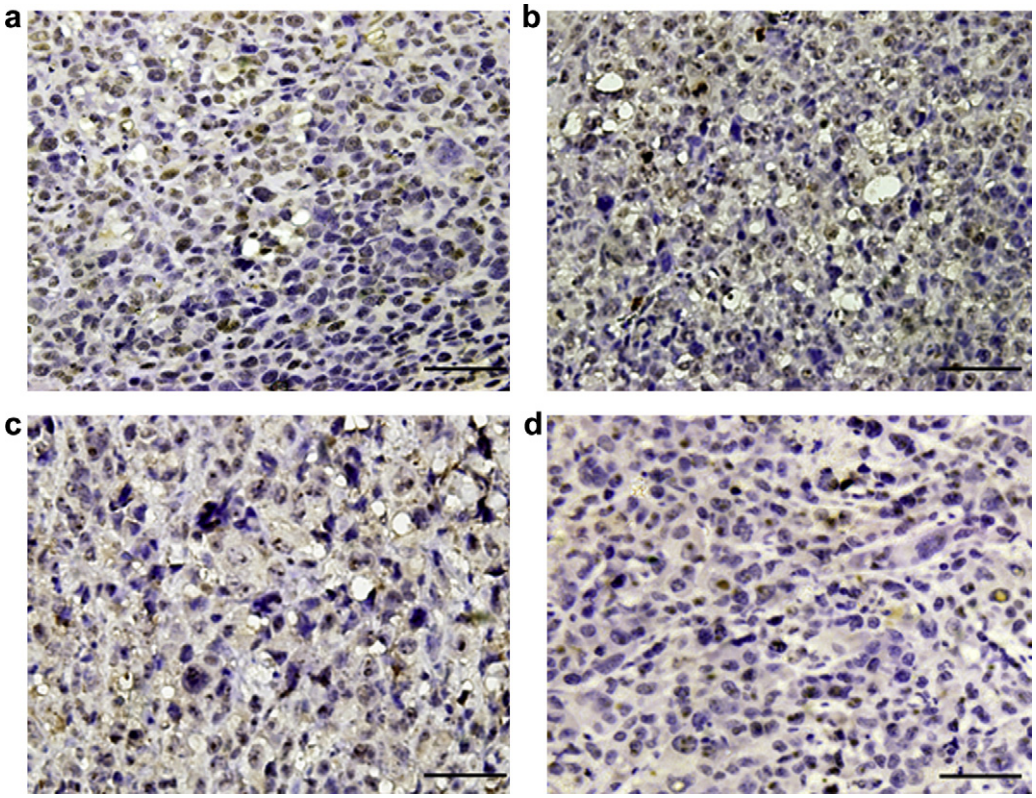

Fig. 9. Typical images of immunohistochemical staining of capase-3 in tumors retrieved on day 14 after treatment with HCPT/PELA fibrous mats (a), free HCPT (b), empty PELA fibers (c) and saline as control (d). Bars represent 5 μm. (For interpretation of the references to color in the text, the reader is referred to the web version of the article.)

10% increase during 14 day treatment with different protocols. As shown in Fig. 7b, the mice experienced a slight weight loss (all less than 10%) after the administration of either free HCPT or empty PELA fibers. The weight loss was recovered gradually and reached 101% and 105% on day 14 after treatment with free HCPT and empty PELA fibers, respectively. Saline treated animals indicated an increase in the body weight during the following period, which was due to the increase in the tumor volume (Fig. 6a). Compared with free HCPT administration, the gradual increase in the body weight in HCPT/PELA group implied the lower systematic toxicity of locally and gradually released HCPT from fibers.

3.8. Histological and immunohistochemical examinations of tumors retrieved

In order to further investigate the antitumor efficacy of HCPT/PELA fibrous mats, HE and caspase-3 immunohistochemical staining were performed on tumor tissues retrieved on day 14 post-treatment. As shown in Fig. 8, in comparison with tissues in groups after saline and empty PELA fiber treatment, larger areas of necrotic region (pink area) can be obviously seen in tumor tissues after treatment with free drug and HCPT/PELA fibers. There were still a large amount of living cells (blue area) can be observed in tumors after treated with saline and empty PELA fibers, and the tumor cells showed obvious nucleolus cleavage and high extent of malignant. The necrotic region in tumors after HCPT/PELA fiber treatment was larger than that of free drug, indicating the effectiveness of sustained release of HCPT from fibers.

The caspases family has been found to play a crucial role in the execution of apoptosis, in which caspase 3 plays a central role (Rana et al., 1998). Fig. 9 shows the positive expression of caspase-3 (brown cells) in tumor tissues. The caspase-3 expressions were stronger in the groups of HCPT/PELA fibers and free HCPT than those of empty PELA fibers and saline. The positive cells were counted from five different areas for each sample, and there were $37.6 \pm 2.5\%$, $18.7 \pm 3.1\%$, $4.7 \pm 0.6\%$ and $3.3 \pm 0.6\%$ for HCPT/PELA fibers, free HCPT, empty PELA fibers and saline, respectively. HCPT/PELA fibers induced significantly higher amount of apoptotic cells ($p < 0.05$), which was attributed to the constant and local delivery HCPT into tumors. The released HCPT can maintain effective curial concentration in tumor tissues for long, and so induced more necrosis and apoptosis, showing excellent antitumor efficacy.

4. Conclusions

Emulsion electrospinning was used to prepare core–sheath structured fibers with core-loading of HCPT. The preferential formation of HPCT/HPCD inclusion complexes resulted in slightly higher initial burst release, significantly faster release and higher matrix degradation rate compared with blend electrospun fibers. The percentage of the lactone form was maintained around 93% after emulsion electrospinning and incubation in buffer solutions due to the core–sheath structure. *In vitro* cytotoxicity assay indicated that over 20 times higher inhibitory activity against HepG2 cells than free HCPT during 72 h incubation. Compared with free HCPT, HCPT-loaded fibers provided significantly higher inhibition effect on the tumor growth after intratumoral implantation, and the primary tumor development after tumor cell injection. By combining the tumor volumes, survival rates and body weight measurement, it was demonstrated that HCPT-loaded fibers had superior *in vivo* antitumor activities to and fewer side effects than free HCPT. The histological and immunohistochemical examinations indicated more necrosis and apoptosis induced by HCPT-loaded fibers. Therefore, this type of nanofibrous implants may be considered promising as drug carries for local treatment of solid tumors.

Acknowledgements

This work was supported by National Natural Science Foundation of China (51073130), and Fundamental Research Funds for the Central Universities (SWJTU11CX126, SWJTU11ZT10, and SWJTU09ZT21).

References

Bibby, D.C., Davies, N.M., Tucker, I.G., 2000. Mechanisms by which cyclodextrins modify drug release from polymeric drug delivery systems. Int. J. Pharm. 197, 1–11.

Bouchard, P., Efron, J., 2010. Management of recurrent rectal cancer. Ann. Surg. Oncol. 17, 1343–1356.

Chakraborty, S., Liao, I.C., Adler, A., Leong, K.W., 2009. Electrohydrodynamics: a facile technique to fabricate drug delivery systems. Adv. Drug Deliv. Rev. 61, 1043–1054.

Crawford, J., Dale, D.C., Lyman, G.H., 2004. Chemotherapy-induced neutropenia: risks, consequences, and new directions for its management. Cancer 100, 228–237.

Cui, W.G., Li, X.H., Zhou, S.B., Weng, J., 2008. Degradation patterns and surface wettability of electrospun fibrous mats. Polym. Degrad. Stabil. 93, 731–738.

Cui, W.G., Li, X.H., Zhu, X.L., Yu, G., Zhou, S.B., Weng, J., 2006. Investigation of drug release and matrix degradation of electrospun poly(DL-lactide) fibers with paracetamol inoculation. Biomacromolecules 7, 1623–1629.

Deng, X.M., Li, X.H., Huang, Z.T., Jia, W.X., Zhang, Y.H., 1999. Optimization of preparative parameters for poly-DL-lactide-poly(ethylene glycol) microspheres with entrapped Vibrio cholera antigens. J. Control. Release 58, 123–131.

Derakhshandeh, K., Erfan, M., Dadashzadeh, S., 2007. Encapsulation of 9-nitrocamptothecin, a novel anticancer drug, in biodegradable nanoparticles: factorial design, characterization and release kinetics. Eur. J. Pharm. Biopharm. 66, 34–41.

Ding, D., Zhu, Z.S., Liu, Q., Wang, J., Hu, Y., Jiang, X.Q., Liu, B.R., 2011. Cisplatin-loaded gelatin-poly(acrylic acid) nanoparticles: synthesis, antitumor efficiency in vivo and penetration in tumors. Eur. J. Pharm. Biopharm. 79, 142–149.

Gabr, A., Kuin, A., Aalders, M., El-Gawly, H., Smets, L.A., 1997. Cellular pharmacokinetics and cytotoxicity of camptothecin and topotecan at normal and acidic pH. Cancer Res. 57, 4811–4816.

Greiner, A., Wendorff, J.H., 2007. Electrospinning: a fascinating method for the preparation of ultrathin fibers. Angew. Chem. Int. Ed. 46, 5670–5703.

Hadjiargyrou, M., Chiu, J.B., 2008. Enhanced composite electrospun nanofiber scaffolds for use in drug delivery. Expert Opin. Drug Deliv. 5, 1093–1106.

Kunii, R., Onishi, H., Machida, Y., 2007. Preparation and antitumor characteristics of PLA/(PEG–PPG–PEG) nanoparticles loaded with camptothecin. Eur. J. Pharm. Biopharm. 67, 9–17.

Li, X.L., Li, R.T., Qian, X.P., Ding, Y.T., Tu, Y.X., Guo, R., Hu, Y., Jiang, X.Q., Guo, W.H., Liu, B.R., 2008. Superior antitumor efficiency of cisplatin-loaded nanoparticles by intratumoral delivery with decreased tumor metabolism rate. Eur. J. Pharm. Biopharm. 70, 726–734.

Li, Y.F., Zhang, R., 1996. Reversed-phase high-performance liquid chromatography method for the simultaneous quantitation of the lactone and carboxylate forms of the novel natural product anticancer agent 10-hydroxycamptothecin in biological fluids and tissues. J. Chromatogr. B: Biomed. Sci. Appl. 686, 257–265.

Liang, D.H., Hsiao, B., Chu, B., 2007. Functional electrospun nanofibrous scaffolds for biomedical applications. Adv. Drug Deliv. Rev. 59, 1392–1412.

Luu, Y.K., Kim, K., Hsiao, B.S., Chu, B., Hadjiargyrou, M., 2003. Development of a nanostructured DNA delivery scaffold via electrospinning of PLGA and PLA-PEG block copolymers. J. Control. Release 89, 341–353.

Opanasopit, P., Ngawhirunpat, T., Chaidedgumjorn, A., Rojanarata, T., Apirakaramwong, A., Phongying, S., Choochottiros, C., Chirachanchai, S., 2006. Incorporation of camptothecin into N-phthaloyl chitosan-g-mPEG self-assembly micellar system. Eur. J. Pharm. Biopharm. 64, 269–276.

Opanasopit, P., Yokoyama, M., Watanabe, M., Kawano, K., Maitani, Y., Okano, T., 2005. Influence of serum and albumins from different species on stability of camptothecin-load micelles. J. Control. Release 104, 313–321.

Pockaj, B.A., Gray, R.J., 2009. Current surgery for breast cancer. Future Oncol. 5, 465–479.

Pradilla, G., Wang, P.P., Gabikian, P., Li, K., Magee, C.A., Walter, K.A., Brem, H., 2006. Local intracerebral administration of paclitaxel with the Paclimer® delivery system: toxicity study in a canine model. J. Neurooncol. 76, 131–138.

Rana, A., Ali, A.M., Begum, Z., Vanaja, J., Khar, A., 1998. Selective involvement of caspase-3 in ceramide induced apoptosis in AK-5 tumor cells. FEBS Lett. 439, 81–84.

Saetern, A.M., Nguyen, N.B., Bauer-Brandl, A., Brandl, M., 2004. Effect of hydroxypropyl-β-cyclodextrin-complexation and pH on solubility of camptothecin. Int. J. Pharm. 284, 61–68.

Sill, T.J., von Recum, H.A., 2008. Electrospinning: applications in drug delivery and tissue engineering. Biomaterials 29, 1989–2006.

Singer, J.W., Bhatt, R., Tulinsky, J., Buhler, K.R., Heasley, E., Klein, P., de Vreis, P., 2001. Water-soluble poly-(L-glutamic acid)-glycamptothecin conjugates enhance camptothecin stability and efficacy in vivo. J. Control. Release 74, 243–247.

Wolinsky, J.B., Liu, R., Walpole, J., Chirieac, R., Colson, Y.L., Grinstaff, M.W., 2010. Prevention of in vivo lung tumor growth by prolonged local delivery of hydroxycamptothecin using poly(ester-carbonate)-collagen composites. J. Control. Release 144, 280–287.

Xie, C.Y., Li, X.H., Luo, X.M., Yang, Y., Cui, W.G., Zou, J., Zhou, S.B., 2010. Release modulation and cytotoxicity of hydroxycamptothecin-loaded electrospun fibers with 2-hydroxypropyl-β-cyclodextrin inoculations. Int. J. Pharm. 391, 55–64.

Xiong, X.B., Huang, Y., Lu, W.L., Zhang, X., Zhang, H., Nagai, T., Zhang, Q., 2005. Enhanced intracellular delivery and improved antitumor efficacy of doxorubicin by sterically stabilized liposomes modified with a synthetic RGD mimetic. J. Control. Release 107, 262–275.

Yang, Y., Li, X.H., Cheng, L., He, S.H., Zou, J., Chen, F., Zhang, Z.B., 2011a. Core-sheath structured fibers with pDNA polyplex loadings for optimal release profile and transfection efficiency as potential tissue engineering scaffolds. Acta Biomater. 7, 2533–2543.

Yang, Y., Li, X.H., Qi, M.B., Zhou, S.B., Weng, J., 2008. Release pattern and structural integrity of lysozyme encapsulated in core-sheath structured poly(DL-lactide) ultrafine fibers prepared by emulsion electrospinning. Eur. J. Pharm. Biopharm. 69, 106–116.

Yang, Y., Xia, T., Zhi, W., Wei, L., Weng, J., Zhang, C., Li, X.H., 2011b. Promotion of skin regeneration in diabetic rats by electrospun core-sheath fibers loaded with basic fibroblast growth factor. Biomaterials 32, 4243–4254.

Yoo, H.S., Kim, T.G., Park, T.G., 2009. Surface-functionalized electrospun nanofibers for tissue engineering and drug delivery. Adv. Drug Deliv. Rev. 61, 1033–1042.

Yu, J.H., Fridrikh, S.V., Rutledge, G.C., 2004. Production of submicrometer diameter fibers by two-fluid electrospinning. Adv. Mater. 16, 1562–1566.

Zhang, L.Y., Yang, M., Wang, Q., Li, Y., Guo, R., Jiang, X.Q., Yang, C.Z., Liu, B.R., 2007. 10-Hydroxycamptothecin loaded nanoparticles: preparation and antitumor activity in mice. J. Control. Release 119, 153–162.

Zhang, Y.Z., Wang, X., Feng, Y., Li, J., Lim, C.T., Ramakrishna, S., 2006. Coaxial electrospinning of (fluorescein isothiocyanate-conjugated bovine serum albumin)-encapsulated poly(ε-caprolactone) nanofibers for sustained release. Biomacromolecules 7, 1049–1057.